Journal of Engineering Mathematics (2025) 151:1
https://doi.org/10.1007/s10665-025-10423-0

The effect of particle–substrate adsorption on the deposition of particles from a thin evaporating sessile droplet

Hannah-May D'Ambrosio[1] · Alexander W. Wray[3] · Stephen K. Wilson[2,3]

Received: 29 May 2024 / Accepted: 7 January 2025

Abstract
A mathematical model for the evaporation of, the flow within, and the deposition from, a thin, pinned sessile droplet undergoing either spatially uniform or diffusion-limited evaporation is formulated and analysed. Specifically, we obtain explicit expressions for the concentration of particles within the bulk of the droplet, and describe the behaviour of the concentration of particles adsorbed onto the substrate as well as the evolution of the masses within the bulk of the droplet, adsorbed onto the substrate, and in the ring deposit that can form at the contact line. In particular, we show that the presence of particle–substrate adsorption suppresses the formation of a ring deposit at the contact line for spatially uniform, but not for diffusion-limited, evaporation. However, in both scenarios, the final adsorbed deposit is more concentrated near to the contact line of the droplet when radial advection due to evaporation dominates particle–substrate adsorption, but is more concentrated near to the centre of the droplet when particle–substrate adsorption dominates radial advection due to evaporation. In addition, in an appendix, we investigate the formation of a ring deposit at the contact line for a rather general form of the local evaporative flux, and show that the presence of particle–substrate adsorption suppresses the formation of the ring deposit that can otherwise occur when the local evaporative flux is non-singular at the contact line.

Keywords Adsorption · Coffee-ring effect · Evaporation · Particle deposition · Sessile droplet

✉ Stephen K. Wilson
sw3197@bath.ac.uk

1 School of Mathematics and Statistics, University of Glasgow, University Place, Glasgow G12 8QQ, UK

2 Department of Mathematical Sciences, University of Bath, Claverton Down, Bath BA2 7AY, UK

3 Department of Mathematics and Statistics, University of Strathclyde, Livingstone Tower, 26 Richmond Street, Glasgow G1 1XH, UK

Published online: 17 February 2025

1 Introduction

The evaporation of sessile droplets occurs in a wide variety of physical contexts, with practical applications in, for example, coating (Layani et al. [1]), chemical and biological assays (Garcia-Cordero and Fan [2]), and inkjet printing (Halls [3]), and has therefore been the subject of extensive analytical, numerical, and experimental investigation in recent years (see, for example, Cazabat and Guéna [4], Erbil [5], Brutin and Starov [6], Giorgiutti-Dauphiné and Pauchard [7], Brutin and Sefiane [8], Gelderblom et al. [9], and Wilson and D'Ambrosio [10], and the references therein). Particular attention has been paid to the well-known "coffee-ring" effect in which a ring deposit forms near to the location of the pinned contact line of a sessile droplet as it evaporates. For the case of a thin, pinned droplet undergoing diffusion-limited evaporation in which the local evaporative flux from the droplet is theoretically infinite at the contact line, Deegan et al. [11] explained that the ring deposit is a consequence of radially outward capillarity-driven flow inside the droplet that transports particles towards its pinned contact line. In their study, Deegan et al. [11] obtained a theoretical prediction for the growth of the ring deposit when radial particle diffusion is neglected. Following Deegan et al. [11], the deposition of particles for an evaporating droplet has been studied in great detail (see, for example, Larson [12], Mampallil and Eral [13], Parsa et al. [14], Zang et al. [15], Kolegov and Barash [16], and Shoa et al. [17], and the references therein). In particular, various authors have extended the basic particle-transport model described by Deegan et al. [11] by, for example, incorporating high concentration effects through particle jamming/gelation (see, for example, Popov [18], Zheng [19], and Kaplan and Mahadevan [20]) and particle diffusion (see, for example, Moore et al. [21]) near to the contact line of the droplet. We note that, for a pinned droplet, the mechanism underlying the coffee-ring effect is surprisingly robust, and local evaporative fluxes that are non-singular, and even zero, at the contact line can also induce a mean flow into the contact line, and hence can also give rise to a ring deposit (see, for example, D'Ambrosio et al. [22]). In particular, spatially uniform evaporation exhibits the same qualitative behaviour of the deposition of particles for a pinned evaporating droplet (see, for example, Boulogne et al. [23] and D'Ambrosio et al. [22]), and, due to its simplicity, is sometimes used to approximate diffusion-limited evaporation (see, for example, Ozawa et al. [24], Man and Doi [25], Zigelman and Manor [26, 27], and Mills [28]).

The shape of the deposit from an evaporating droplet is determined by both the flow and particle interactions present within the droplet. In particular, previous authors have reported a qualitative change in the deposition from an evaporating droplet by promoting particle–free-surface, particle–particle, and particle–substrate interactions through the addition of polymers (Kim et al. [29]), proteins (Devineau et al. [30]), and surfactants (Anyfantakis et al. [31]), by changing the acidity of the fluid (Bhardwaj et al. [32]), or by altering properties of the particles within the droplet, such as particle concentration (Lee et al. [33]), material (Anyfantakis [34]), shape (Yunker [35, 36]), and size (Ryu et al. [37]).

A number of theoretical investigations of the effect of particle interactions on the deposition from an evaporating droplet have been performed (see, for example, Widjaja and Harris [38], Siregar et al. [39], Crivoi and Duan [40], Crivoi et al. [41], Zigelman

and Manor [26, 27], Sung et al. [42], Ren et al. [43], and Erdem et al. [44]). In particular, Widjaja and Harris [38] and Sung et al. [42] numerically investigated the deposition of particles from a pinned droplet undergoing diffusion-limited evaporation and identified a variety of different final deposition patterns, including a ring deposit and an almost uniform deposit, depending upon the relative strength of particle advection, particle diffusion and particle–substrate adsorption. Sung et al. [42] also considered the effect of particle–substrate desorption. Siregar et al. [39] numerically investigated the evolution of, and the deposition from, both a pinned and an unpinned droplet undergoing diffusion-limited evaporation, including the effects of particle–substrate adsorption and desorption. In particular, they observed a transition from a ring deposit when the contact line is pinned to a deposit that is more concentrated near to the centre of the droplet when the contact line is unpinned. Crivoi and Duan [40], Crivoi et al. [41], and Ren et al. [43] used a Monte Carlo method to study the transition from a ring deposit to a more uniform deposit from a pinned droplet. In particular, Crivoi and Duan [40] showed that, at least according to the model they employed, particle–free-surface adsorption, long-range particle–particle attraction, and Marangoni effects must all be present in order to suppress the formation of a ring deposit near to the contact line of the droplet, again illustrating the robustness of the coffee-ring effect. Zigelman and Manor [26, 27] used a combination of numerical and analytical techniques to study the effect of particle–substrate adsorption and particle–particle coagulation on the deposition from a thin, pinned droplet undergoing spatially uniform evaporation. In particular, Zigelman and Manor [26] identified a critical rate of particle–substrate adsorption at which the final deposit is uniform, and observed a transition from a ring deposit below this threshold to a deposit that is more concentrated near to the centre of the droplet above it. Recently, Erdem et al. [44] numerically investigated the evolution of, and deposition from, a thin two-dimensional droplet undergoing kinetically limited (i.e. one-sided) evaporation. In particular, they analysed the effect of contact-line motion, Marangoni effects, evaporative effects, particle–substrate adsorption rate, and particle diffusion on the final deposition pattern, and recovered several of the behaviours observed by previous authors.

Thus, while there have been previous investigations of the effect of particle interactions on the deposition of particles from an evaporating droplet, there are no analytical studies for the effect of particle–substrate adsorption on the deposition from a droplet undergoing diffusion-limited evaporation. The aim of the present work is to rectify this omission. Specifically, in Sect. 2, we will formulate a mathematical model for the evaporation of, the flow within, and the deposition from, a thin, pinned sessile droplet undergoing either spatially uniform or diffusion-limited evaporation. In Sect. 3, we will obtain explicit expressions for the concentration of particles within the bulk of the droplet, and describe the behaviour of the concentration of particles adsorbed onto the substrate, the evolution of the masses within the bulk of the droplet, adsorbed onto the substrate, and in the ring deposit that can form at the contact line. In Appendix A, we investigate the formation of a ring deposit at the contact line for a rather general form of the local evaporative flux.

2 Problem formulation

Consider the evaporation of a small, thin, axisymmetric, sessile droplet on a planar substrate with a pinned circular contact line with constant radius $\hat{R}_0$. We assume that the suspension of particles within the droplet is sufficiently dilute that the presence of the particles does not affect the flow, and refer the description to cylindrical polar coordinates $\hat{r}$ and $\hat{z}$ with $O\hat{z}$ along the axis of the droplet, perpendicular to the substrate at $\hat{z} = 0$. The contact angle, free surface, and volume of the droplet are denoted by $\hat{\theta} = \hat{\theta}(\hat{t})$, $\hat{h} = \hat{h}(\hat{r}, \hat{t})$, and $\hat{V} = \hat{V}(\hat{t})$, respectively, where $\hat{t}$ denotes time. The initial values of $\hat{\theta}$ and $\hat{V}$ at $\hat{t} = 0$ are denoted by $\hat{\theta}_0$ and $\hat{V}_0$, respectively. After the droplet is deposited onto the substrate at an initial time $\hat{t} = 0$, its volume decreases until it has completely evaporated, i.e. until $\hat{V}(\hat{t}_{\text{lifetime}}) = 0$, where $\hat{t}_{\text{lifetime}}$ denotes the lifetime of the droplet.

We consider situations in which the droplet is thin, corresponding to a small value of the initial contact angle of the droplet $\hat{\theta}_0 \ll 1$. We consider droplets that are sufficiently small such that the effect of gravity is negligible, corresponding to a small value of the appropriately defined Bond number

$$\text{Bo} = \frac{\hat{\rho}\hat{g}\hat{R}_0}{\hat{\sigma}} \ll 1, \tag{1}$$

where $\hat{\rho}$ and $\hat{\sigma}$ are the constant density and surface tension of the fluid, respectively, and $\hat{g}$ denotes the magnitude of acceleration due to gravity. We now consider the coupled problems for the evaporation of, the flow within, and the deposition from, the droplet, in turn.

2.1 The evaporative problem

According to the basic diffusion-limited model (see, for example, Murisic and Kondic [45] and Wilson and D'Ambrosio [10]), the quasi-static concentration of vapour in the atmosphere, denoted by $\hat{c} = \hat{c}(\hat{r}, \hat{z}, \hat{t})$, satisfies Laplace's equation $\hat{\nabla}^2\hat{c} = 0$ subject to conditions of complete saturation on the free surface of the droplet and of no flux of vapour through the unwetted part of the substrate.

We scale and non-dimensionalise variables appropriately for the atmosphere according to

$$\hat{r} = \hat{R}_0 r, \hat{z} = \hat{R}_0\bar{z}, \hat{V} = \hat{\theta}_0\hat{R}_0^3 V, \hat{c} = \hat{c}_\infty + (\hat{c}_{\text{sat}} - \hat{c}_\infty)c, \hat{J} = \hat{J}_{\text{ref}} J, \hat{t} = \hat{t}_{\text{ref}} t, \tag{2}$$

where $\hat{c}_{\text{sat}}$ and $\hat{c}_\infty$ are the constant saturation concentration and far-field concentration of vapour, respectively, and $\hat{J}_{\text{ref}}$ and $\hat{t}_{\text{ref}}$ are the characteristic scale of the local evaporative mass flux from the droplet, denoted by $\hat{J} = \hat{J}(\hat{r})$, and the characteristic timescale, respectively, which, for diffusion-limited evaporation, are given by

$$\hat{J}_{\text{ref}} = \frac{\hat{D}(\hat{c}_{\text{sat}} - \hat{c}_\infty)}{\hat{R}_0}, \quad \hat{t}_{\text{ref}} = \frac{\hat{\rho}\hat{\theta}_0\hat{R}_0^2}{\hat{D}(\hat{c}_{\text{sat}} - \hat{c}_\infty)}, \tag{3a,b}$$

in which $\hat{D}$ is the constant diffusion coefficient of vapour in the atmosphere. Note that the scaling for $\hat{z}$ in the atmosphere that appears in (2) differs from that for $\hat{z}$ in the droplet introduced subsequently.

For a thin droplet the exact solution to the basic diffusion-limited model is well known (see, for example, Wilson and Duffy [46]) and leads to the familiar expression for J, namely

$$J = \frac{2}{\pi \left(1 - r^2\right)^{1/2}}. \tag{4}$$

Integrating J over the free surface of the droplet gives the total evaporative mass flux from the droplet, denoted by F and non-dimensionalised by $\hat{D}(\hat{c}_{\mathrm{sat}} - \hat{c}_{\infty})\hat{R}_0$. In particular, for a thin droplet, this is given by

$$F = 2\pi \int_0^1 J\, r \, \mathrm{d}r = 4. \tag{5}$$

The volume of the droplet evolves according to the global mass-conservation condition

$$\frac{\mathrm{d}V}{\mathrm{d}t} = -F. \tag{6}$$

In the present work, we will also consider a spatially uniform evaporative flux that is independent of the radial position r defined by

$$J \equiv \frac{4}{\pi}, \tag{7}$$

which, when integrated over the free surface of the droplet, has the same value of $F = 4$ as that for diffusion-limited evaporation given by (5). We will compare the deposition of particles from a droplet undergoing either spatially uniform or diffusion-limited evaporation in Sect. 3.

2.2 The hydrodynamic problem

The velocity and pressure within the droplet, denoted by $\hat{\mathbf{u}} = \left(\hat{u}(\hat{r}, \hat{z}, \hat{t}), 0, \hat{w}(\hat{r}, \hat{z}, \hat{t})\right)$ and $\hat{p} = \hat{p}(\hat{r}, \hat{z}, \hat{t})$, respectively, satisfy the usual mass-conservation and Stokes equations subject to no-slip and no-penetration conditions on the substrate and stress and kinematic conditions on the free surface of the droplet.

We scale and non-dimensionalise variables appropriately for the droplet according to

$$\begin{gathered} \hat{r} = \hat{R}_0 r, \quad \hat{z} = \hat{\theta}_0 \hat{R}_0 z, \quad \hat{h} = \hat{\theta}_0 \hat{R}_0 h, \quad \hat{u} = \hat{u}_{\mathrm{ref}} u, \\ \hat{w} = \hat{\theta}_0 \hat{u}_{\mathrm{ref}} w, \quad \hat{p} - \hat{p}_{\mathrm{a}} = \frac{\hat{\gamma}\hat{\theta}_0}{\hat{R}_0} p, \end{gathered} \tag{8}$$

where $\hat{\gamma}$ is the constant coefficient of surface tension at the free surface of the droplet, $\hat{p}_{\mathrm{a}}$ is the constant atmospheric pressure, and $\hat{u}_{\mathrm{ref}}$ is the characteristic radial velocity

scale given by

$$\hat{u}_{\mathrm{ref}} = \frac{\hat{R}_0}{\hat{t}_{\mathrm{ref}}} = \frac{\hat{D}(\hat{c}_{\mathrm{sat}} - \hat{c}_\infty)}{\hat{\rho}\hat{\theta}_0\hat{R}_0}. \tag{9}$$

We consider situations in which the capillary effects are sufficiently strong that the droplet evolves quasi-statically, corresponding to sufficiently small values of the capillary number Ca defined by

$$\mathrm{Ca} = \frac{\hat{\mu}\hat{u}_{\mathrm{ref}}}{\hat{\gamma}\hat{\theta}_0^3} = \frac{\hat{\mu}\hat{D}(\hat{c}_{\mathrm{sat}} - \hat{c}_\infty)}{\hat{\gamma}\hat{\rho}\hat{\theta}_0^4\hat{R}_0}, \tag{10}$$

in which $\hat{\mu}$ is the constant dynamic viscosity of the fluid. More specifically, we assume that $\hat{\theta}_0^2, \mathrm{Bo} \ll \mathrm{Ca} \ll 1$ and therefore seek an asymptotic solution for the pressure p in the form

$$p = p^{(0)} + \mathrm{Ca}\, p^{(1)} + O(\hat{\theta}_0^2, \mathrm{Bo}, \mathrm{Ca}^2) \tag{11}$$

(see, for example, D'Ambrosio et al. [22]). Note that, as we shall see, the first-order pressure term $p^{(1)}$ is the only term required beyond leading order to describe the flow within and the deposition from an evaporating droplet, and so, for clarity, we omit the "(0)" superscript on all other leading-order quantities.

At leading order in $\mathrm{Ca} \ll 1$, the Stokes equation reduces to $\partial p^{(0)}/\partial r = \partial p^{(0)}/\partial z = 0$, i.e. $p^{(0)} = p^{(0)}(t)$ is independent of r and z, and hence is determined simply by the normal stress condition on the free surface of the droplet, namely

$$p^{(0)} = -\frac{1}{r}\frac{\partial}{\partial r}\left(r\frac{\partial h}{\partial r}\right). \tag{12}$$

The leading-order free-surface profile $h = h(r,t)$ therefore takes the familiar paraboloidal form

$$h = \frac{\theta\left(1 - r^2\right)}{2}, \tag{13}$$

and the leading-order volume is given by

$$V = 2\pi\int_0^1 h\, r\, \mathrm{d}r = \frac{\pi\theta}{4}. \tag{14}$$

Substituting the expressions for F and V given by (5) and (14), respectively, into (6) and solving for θ yields the well-known solution for the evolution of a thin, pinned droplet undergoing diffusion-limited evaporation, namely

$$\theta = 1 - \frac{16}{\pi}t, \quad V = \frac{\pi}{4}\left(1 - \frac{16}{\pi}t\right) \tag{15a,b}$$

(see, for example, Wilson and Duffy [46]). Note that, since they have the same value of the total evaporative flux $F = 4$, the solution (15) also describes the evolution of a droplet undergoing spatially uniform evaporation given by (7). Setting either $\theta = 0$ or

$V = 0$ in (15) shows that, for both diffusion-limited and spatially uniform evaporation, the lifetime of the droplet is given by

$$t_{\text{lifetime}} = \frac{\pi}{16}. \tag{16}$$

The mass-conservation equation is

$$\frac{1}{r}\frac{\partial (ru)}{\partial r} + \frac{\partial w}{\partial z} = 0, \tag{17}$$

and at first order in $\text{Ca} \ll 1$, the Stokes equation reduces to

$$\frac{\partial^2 u}{\partial z^2} = \frac{\partial p^{(1)}}{\partial r}, \quad 0 = \frac{\partial p^{(1)}}{\partial z}, \tag{18}$$

which is to be solved subject to no-slip and no-penetration conditions on the substrate, i.e. $u(r, 0, t) = w(r, 0, t) = 0$, and the tangential stress condition $\partial u/\partial z = 0$ on the free surface of the droplet (see, for example, Wray et al. [47]). The kinematic condition may be expressed by

$$\frac{\partial h}{\partial t} + \frac{1}{r}\frac{\partial (rQ)}{\partial r} = -J, \tag{19}$$

where $Q = Q(r, t)$ is the local radial volume flux, defined by

$$Q = \int_0^h u \, \mathrm{d}z = h\bar{u}, \tag{20}$$

and $\bar{u} = \bar{u}(r, t)$ is the depth-averaged radial velocity, defined by

$$\bar{u} = \frac{1}{h}\int_0^h u \, \mathrm{d}z = \frac{Q}{h}. \tag{21}$$

As we shall see in Sect. 2.3, knowledge of $\bar{u}$ is sufficient to describe the evolution of the concentration of particles at leading order, and hence the evolution of the mass of particles within the droplet.

For future reference, we note that the kinematic condition (19) may be rearranged and integrated with respect to r to yield

$$Q = -\frac{1}{r}\int_0^r \left(\frac{\partial h}{\partial t} + J\right)\tilde{r} \, \mathrm{d}\tilde{r}. \tag{22}$$

2.3 The particle-transport problem

The concentration of particles per unit volume within the bulk of the droplet, denoted by $\hat{\phi} = \hat{\phi}(\hat{r}, \hat{z}, \hat{t})$, satisfies an advection–diffusion equation subject to an adsorption condition on the substrate and a condition of conservation of particles at the free surface of the droplet.

Non-dimensionalising according to $\hat{\phi} = \hat{\phi}_{\text{ref}}\phi$, where $\hat{\phi}_{\text{ref}}$ is the spatial average of the initial concentration of particles within the droplet, shows that $\phi = \phi(r, z, t)$ satisfies

$$\text{Pe}^* \left(\frac{\partial \phi}{\partial t} + u \frac{\partial \phi}{\partial r} + w \frac{\partial \phi}{\partial z} \right) = \hat{\theta}_0^2 \frac{1}{r} \frac{\partial}{\partial r} \left(r \frac{\partial \phi}{\partial r} \right) + \frac{\partial^2 \phi}{\partial z^2}, \tag{23}$$

where Pe^* $(= \hat{\theta}_0^2 \text{Pe})$ is the appropriately defined reduced particle Péclet number that characterises the ratio of advective and diffusive particle-transport timescales, namely

$$\text{Pe}^* = \frac{\hat{\theta}_0^2 \hat{R}_0 \hat{u}_{\text{ref}}}{\hat{D}_{\text{p}}} = \frac{\hat{\theta}_0 \hat{D} \left(\hat{c}_{\text{sat}} - \hat{c}_\infty \right)}{\hat{\rho} \hat{D}_{\text{p}}}, \tag{24}$$

in which $\hat{D}_{\text{p}}$ is the constant diffusivity of the particles in the fluid.

The adsorption of suspended particles onto a solid substrate is a complicated process that is driven by short-range interactions between the particles and the substrate and can depend on a variety of physical effects, including hydrodynamic, van der Waals, and electrostatic forces (see, for example, Elimelech et al. [48] and Adamczyk [49]). In the present work, we adopt a simple phenomenological model for the particle–substrate adsorption that simply states that adsorption is irreversible and that the diffusive flux of particles onto the substrate is proportional to the local concentration of particles on the substrate with the constant adsorption coefficient $\hat{k}_{\text{a}}$, i.e.

$$\hat{D}_{\text{p}} \frac{\partial \hat{\phi}}{\partial \hat{z}} = \hat{k}_{\text{a}} \hat{\phi} \quad \text{on} \quad \hat{z} = 0, \tag{25}$$

(see, for example, Widjaja and Harris [38] and Zigelman and Manor [26, 27]). The non-dimensional form of (25) is

$$\frac{\partial \phi}{\partial z} = \text{Pe}^* \text{Da}\, \phi \quad \text{on} \quad z = 0, \tag{26}$$

where Da $(= O(1))$ is the appropriately defined Damköhler number that characterises the ratio of particle–substrate adsorption and advective timescales, namely

$$\text{Da} = \frac{\hat{k}_{\text{a}} \hat{t}_{\text{ref}}}{\hat{\theta}_0 \hat{R}_0} = \frac{\hat{\rho} \hat{k}_{\text{a}} \hat{R}_0}{\hat{D} (\hat{c}_{\text{sat}} - \hat{c}_\infty)}. \tag{27}$$

Conservation of particles at the free surface of the droplet requires that

$$\hat{D}_{\text{p}} \nabla \phi \cdot \hat{\mathbf{n}} = \frac{\hat{J} \hat{\phi}}{\hat{\rho}} \quad \text{on} \quad \hat{z} = \hat{h}, \tag{28}$$

where $\hat{\mathbf{n}}$ is the unit outward normal to the free surface (see, for example, Zigelman and Manor [26, 27]).[1] The non-dimensional form of (28) is

$$\frac{1}{\sqrt{1+\hat{\theta}_0^2(\partial h/\partial r)^2}}\left(\frac{\partial \phi}{\partial z}-\hat{\theta}_0^2\frac{\partial h}{\partial r}\frac{\partial \phi}{\partial r}\right)=\mathrm{Pe}^* J\phi \quad \text{on} \quad z=h. \tag{29}$$

The concentration of particles per unit area adsorbed onto the substrate within the footprint of the droplet, denoted by $\phi_\mathrm{s}=\phi_\mathrm{s}(r,t)$ and non-dimensionalised by $\hat{\theta}_0\hat{R}_0\hat{\phi}_\mathrm{ref}$, satisfies

$$\frac{\partial \phi_\mathrm{s}}{\partial t}=\mathrm{Da}\,\phi(r,0,t). \tag{30}$$

The final adsorbed deposit, i.e. the adsorbed deposit at $t=t_\mathrm{lifetime}$, is denoted by $\phi_{\mathrm{s,\,lifetime}}=\phi_{\mathrm{s,\,lifetime}}(r)$ and given by $\phi_{\mathrm{s,\,lifetime}}=\phi_\mathrm{s}(r,t_\mathrm{lifetime})$.

We consider situations in which the vertical diffusion of particles within the droplet is fast relative to the rate of evaporation and particle–substrate adsorption, corresponding to small values of Pe*. More specifically, we assume that $\hat{\theta}_0^2 \ll \mathrm{Pe}^* \ll 1$ and therefore seek an asymptotic solution for ϕ in the form

$$\phi=\phi^{(0)}+\mathrm{Pe}^*\phi^{(1)}+O\left(\hat{\theta}_0^2,\mathrm{Pe}^{*2}\right) \tag{31}$$

(see, for example, Wray et al. [47] and D'Ambrosio et al. [22]).

At leading order in $\mathrm{Pe}^* \ll 1$, equation (23) reduces to $\partial^2\phi^{(0)}/\partial z^2=0$, subject to $\partial\phi^{(0)}/\partial z=0$ on the substrate and the free surface of the droplet, and hence $\phi^{(0)}=\phi^{(0)}(r,t)$ is independent of z.

At first order in $\mathrm{Pe}^* \ll 1$, equations (23), (26), and (29) reduce to

$$\frac{\partial^2\phi^{(1)}}{\partial z^2}=\frac{\partial\phi^{(0)}}{\partial t}+u\frac{\partial\phi^{(0)}}{\partial r} \tag{32}$$

subject to

$$\frac{\partial\phi^{(1)}}{\partial z}=\mathrm{Da}\,\phi^{(0)} \quad \text{on} \quad z=0 \tag{33}$$

and

$$\frac{\partial\phi^{(1)}}{\partial z}=J\phi^{(0)} \quad \text{on} \quad z=h. \tag{34}$$

Integrating (32) with respect to z from 0 to h, subject to the boundary conditions (33) and (34), and dropping the superscript "(0)" on ϕ for clarity, yields the following governing equation for the leading-order concentration of particles $\phi=\phi(r,t)$,

$$\frac{\partial\phi}{\partial t}+\bar{u}\frac{\partial\phi}{\partial r}=\frac{(J-\mathrm{Da})\phi}{h}, \tag{35}$$

[1] Note that the conditions of conservation of particles at the free surface of the droplet given in equation (13) of [38] and equation (9) of [42] both contain (different) minor typographical errors that fortunately do not appear to affect the numerical results presented in either of these works.

where $\bar{u}$ is given by (21). As mentioned in Sect. 2.3, determining the leading-order evolution of the concentration of particles from (35) only requires knowledge of $\bar{u}$, not u and w. Setting $\mathrm{Da} = 0$ in (35) recovers the familiar governing equation for ϕ when there is no flux of particles onto the substrate, i.e. in the absence of particle–substrate adsorption (see, for example, Deegan et al. [11] and Wray et al. [47, 50]). From (30), the leading-order concentration of particles adsorbed onto the substrate is then given simply by $\partial\phi_\mathrm{s}/\partial t = \mathrm{Da}\,\phi$, which has the following solution in terms of the temporal integral of ϕ,

$$\phi_\mathrm{s} = \mathrm{Da}\int_0^t \phi(r,\tilde{t})\,\mathrm{d}\tilde{t}. \tag{36}$$

Equation (35) may be put into characteristic form, i.e.

$$\frac{\mathrm{d}\phi}{\mathrm{d}t} = \frac{(J-\mathrm{Da})\phi}{h} \quad \text{on the characteristics determined by} \quad \frac{\mathrm{d}r}{\mathrm{d}t} = \bar{u} = \frac{Q}{h}, \tag{37}$$

and solved subject to a prescribed initial concentration $\phi(r,0) = \phi_0(r)$ using the method of characteristics. In particular, following D'Ambrosio et al. [22], the characteristic equations (37) may be expressed as

$$\frac{\mathrm{d}r}{\mathrm{d}\theta} = \frac{\mathrm{d}r/\mathrm{d}t}{\mathrm{d}\theta/\mathrm{d}t} = \frac{Q}{\theta\partial h/\partial t}, \quad \frac{\mathrm{d}\phi}{\mathrm{d}r} = \frac{\mathrm{d}\phi/\mathrm{d}t}{\mathrm{d}r/\mathrm{d}t} = \frac{(J-\mathrm{Da})\phi}{Q}, \tag{38a,b}$$

which can be integrated to yield

$$\log\theta = \int_{r_0}^{r} \frac{\partial h/\partial t}{Q}\,\mathrm{d}\tilde{r}, \quad \log\frac{\phi}{\phi_0} = \int_{r_0}^{r} \frac{J-\mathrm{Da}}{Q}\,\mathrm{d}\tilde{r}, \tag{39a,b}$$

where r_0 satisfies $0 \le r_0 \le 1$ and is determined by solving (39a). Adding (39a) and (39b) and using (19) yields

$$\log\theta + \log\frac{\phi}{\phi_0} = \int_{r_0}^{r} \frac{\partial h/\partial t + J - \mathrm{Da}}{Q}\,\mathrm{d}\tilde{r} = -\int_{r_0}^{r} \frac{1}{\tilde{r}Q}\frac{\partial(\tilde{r}Q)}{\partial\tilde{r}}\,\mathrm{d}\tilde{r} - \int_{r_0}^{r}\frac{\mathrm{Da}}{Q}\,\mathrm{d}\tilde{r}, \tag{40}$$

and therefore

$$\log\theta + \log\frac{\phi}{\phi_0} = \log\frac{r_0 Q(r_0,t)}{r\,Q(r,t)} - \int_{r_0}^{r}\frac{\mathrm{Da}}{Q}\,\mathrm{d}\tilde{r}. \tag{41}$$

Hence, the implicit solution of (35) can be expressed as

$$\log\theta = -\frac{8}{\pi}\int_{r_0}^{r}\frac{1-r^2}{Q}\,\mathrm{d}\tilde{r}, \quad \frac{\phi}{\phi_0} = \frac{r_0 Q(r_0,t)}{\theta r\,Q(r,t)}\exp\left(-\int_{r_0}^{r}\frac{\mathrm{Da}}{Q}\,\mathrm{d}\tilde{r}\right). \tag{42a,b}$$

Setting $\mathrm{Da} = 0$ in (42) recovers the corresponding solution in the absence of particle–substrate adsorption obtained by D'Ambrosio et al. [22].

The mass of particles per unit area within the droplet is ϕh, and so the mass of particles in the bulk of the droplet as it evaporates, denoted by $M_\mathrm{drop} = M_\mathrm{drop}(t)$ and

non-dimensionalised by $\hat{\theta}_0 \hat{R}_0^3 \hat{\phi}_{\mathrm{ref}}$, is given by

$$M_{\mathrm{drop}} = 2\pi \int_0^1 \phi\, h\, r \, \mathrm{d}r. \tag{43}$$

The initial mass of particles in the droplet is $M_{\mathrm{drop}}(0) = M_0$, where

$$M_0 = 2\pi \int_0^1 \phi_0(r)\, h(r, 0)\, r \, \mathrm{d}r. \tag{44}$$

For the present model, during the evaporation of the droplet particles are lost from the bulk of the droplet due to adsorption of particles onto the substrate and/or the flux of particles into the contact line. Therefore, during the evaporation the total mass of particles is divided between the mass of particles in the bulk of the droplet, the mass of particles adsorbed onto the substrate, and the mass of particles in the ring deposit that can form at the contact line of the droplet.

The mass of particles that have been adsorbed onto the substrate, denoted by $M_{\mathrm{sub}} = M_{\mathrm{sub}}(t)$ and also non-dimensionalised by $\hat{\theta}_0 \hat{R}_0^3 \hat{\phi}_{\mathrm{ref}}$, is given by

$$M_{\mathrm{sub}} = 2\pi \int_0^1 \phi_{\mathrm{s}}\, r \, \mathrm{d}r. \tag{45}$$

The mass flux of particles from the bulk of the droplet into the contact line is $\lim_{r \to 1^-} 2\pi(\phi\, Q\, r)$, and so the mass of particles in the ring deposit that can form at the contact line, denoted by $M_{\mathrm{ring}} = M_{\mathrm{ring}}(t)$ and also non-dimensionalised by $\hat{\theta}_0 \hat{R}_0^3 \hat{\phi}_{\mathrm{ref}}$, is given by

$$M_{\mathrm{ring}} = 2\pi \int_0^t \lim_{r \to 1^-} (\phi\, Q\, r) \, \mathrm{d}\tilde{t}. \tag{46}$$

It is straightforward to show that

$$\frac{\mathrm{d}}{\mathrm{d}t} \left(M_{\mathrm{drop}} + M_{\mathrm{sub}} + M_{\mathrm{ring}} \right) = 0, \tag{47}$$

i.e. that the total mass of particles is conserved.

For simplicity, in the remainder of the present work we take the initial concentration of particles in the bulk of the droplet to be spatially uniform such that $\phi_0(r) \equiv 1$. In this case, the initial mass of particles within the droplet given by (44) is simply $M_0 = \pi/4$.

3 Deposition from an evaporating droplet

We will now determine the deposition of particles from a droplet undergoing either spatially uniform or diffusion-limited evaporation.

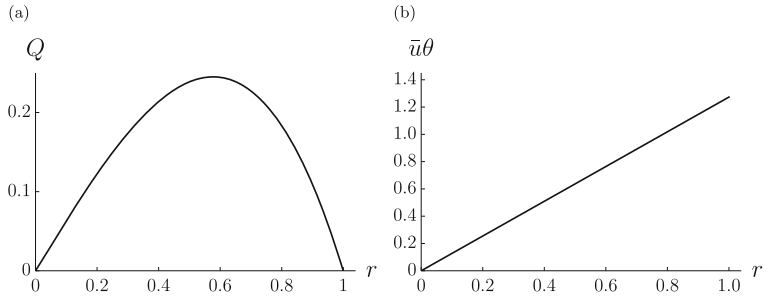

Fig. 1 **a** Q given by (48) and **b** $\bar{u}\theta$ given by (49) plotted as functions of r for a droplet undergoing spatially uniform evaporation

3.1 Spatially uniform evaporation

Substituting the expressions for J and h given by (7) and (13), respectively, into (22) and evaluating the integral yields the familiar expressions for Q, and hence $\bar{u}$, for a thin droplet undergoing spatially uniform evaporation,

$$Q = \frac{2r}{\pi}\left(1 - r^2\right) \tag{48}$$

and

$$\bar{u} = \frac{4r}{\pi\theta} \tag{49}$$

(see, for example, Boulogne et al. [23] and D'Ambrosio et al. [22]). Figure 1 shows Q and $\bar{u}\theta$ (both of which are independent of t) plotted as functions of r.

Substituting the expression for Q given by (48) into (42) and evaluating the integrals yields

$$r_0 = \theta^{1/4} r, \quad \phi = \frac{1}{\theta}\left(\frac{r_0^2}{r^2}\right)^{1+\pi \mathrm{Da}/4}\left(\frac{1 - r_0^2}{1 - r^2}\right)^{1-\pi \mathrm{Da}/4}, \tag{50a,b}$$

and using (50a) to eliminate r_0 from (50b) yields an explicit expression for the concentration of particles within a droplet undergoing spatially uniform evaporation, namely

$$\phi = \left(\frac{\theta^{-1/2} - r^2}{1 - r^2}\right)^{1-\pi \mathrm{Da}/4}. \tag{51}$$

Equation (51) is equivalent to the corresponding expression obtained by Zigelman and Manor [26] [their equation (21)] in which J is spatially uniform and defined by $J \equiv 1$, and setting $\mathrm{Da} = 0$ in (51) recovers the solution for ϕ in the absence of particle–substrate adsorption (see, for example, Zheng [19]).

Figures 2 and 3 show ϕ given by (51) plotted as a function of r at various times for (a) $\mathrm{Da} = 2/\pi$ (typical of $0 \leq \mathrm{Da} < 4/\pi$) and (b) $\mathrm{Da} = 6/\pi$ (typical of $\mathrm{Da} > 4/\pi$), and as a function of r at $t = t_{\mathrm{lifetime}}/2 = \pi/32$ for various values of Da, respectively. Note

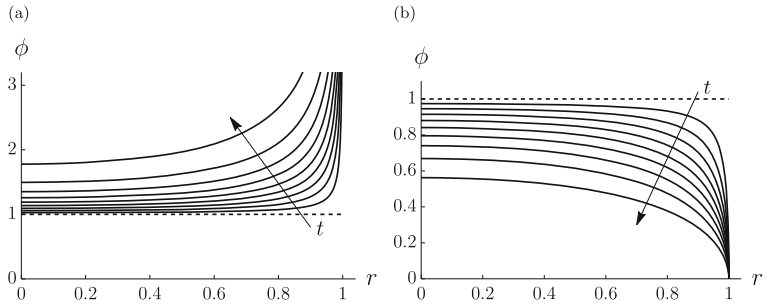

Fig. 2 The concentration of particles within the droplet ϕ given by (51) plotted as a function of r at times $t = (0, 1/10, \ldots, 9/10) \times t_{\text{lifetime}}$ for a droplet undergoing spatially uniform evaporation when **a** $\text{Da} = 2/\pi$ and **b** $\text{Da} = 6/\pi$. The dashed lines correspond to the initial concentration $\phi \equiv 1$ at $t = 0$, and the arrows indicate the direction of increasing t

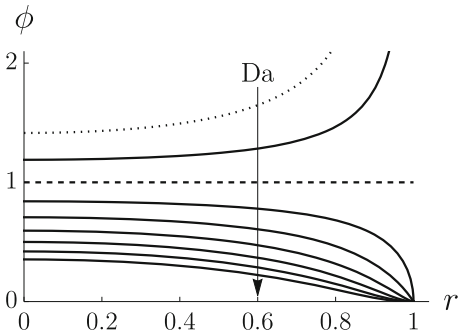

Fig. 3 The concentration of particles within the droplet ϕ given by (51) plotted as a function of r at $t = t_{\text{lifetime}}/2 = \pi/32$ for a droplet undergoing spatially uniform evaporation when $\text{Da} = (0, 1/2, \ldots, 4) \times 4/\pi$. The dotted and dashed lines correspond to $\text{Da} = 0$ and $\text{Da} = 4/\pi$, respectively, and the arrow indicates the direction of increasing Da

that $\phi \equiv 1$ when $\text{Da} = 4/\pi$, and so, for brevity, this special case is omitted from Fig. 2. In particular, Figs. 2 and 3 illustrate that the behaviour of ϕ is qualitatively different for $0 \leq \text{Da} < 4/\pi$, $\text{Da} = 4/\pi$, and $\text{Da} > 4/\pi$. Specifically, for $0 \leq \text{Da} < 4/\pi$, ϕ is a monotonically increasing function of r that takes its minimum value at $r = 0$ and is singular at the contact line according to $\phi = O\left((1-r)^{-(1-\pi\text{Da}/4)}\right) \to \infty$, and is a monotonically increasing function of t. For $\text{Da} = 4/\pi$, as previously mentioned, ϕ remains spatially uniform and constant and is given by $\phi \equiv 1$. For $\text{Da} > 4/\pi$, ϕ is a monotonically decreasing function of r that takes its maximum value at $r = 0$ and goes to zero at the contact line according to $\phi = O\left((1-r)^{-(1-\pi\text{Da}/4)}\right) \to 0^+$, and is a monotonically decreasing function of t.

Substituting the solution for ϕ given by (51) into (36) and evaluating the integral yields an explicit expression for the concentration of particles adsorbed onto the substrate ϕ_s, namely

$$\phi_s = \frac{\pi\text{Da}\left(1-r^2\right)^{-(1-\pi\text{Da}/4)}}{8r^{2(1+\pi\text{Da}/4)}}\left[B_{r^2}\left(1+\frac{\pi\text{Da}}{4}, 2-\frac{\pi\text{Da}}{4}\right) - B_{\theta^{1/2}r^2}\left(1+\frac{\pi\text{Da}}{4}, 2-\frac{\pi\text{Da}}{4}\right)\right], \tag{52}$$

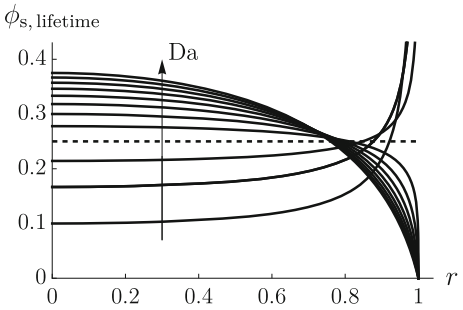

Fig. 4 The concentration of particles adsorbed onto the substrate at the end of the evaporation $\phi_{\text{s, lifetime}}$ given by (54) plotted as a function of r for a droplet undergoing spatially uniform evaporation when $\text{Da} = (1/4, 1/2, \ldots, 3) \times 4/\pi$. The dashed line corresponds to $\text{Da} = 4/\pi$, and the arrow indicates the direction of increasing Da

where $B_z(a, b)$ denotes the incomplete Beta function defined by

$$B_z(a, b) = \int_0^z x^{a-1}(1-x)^{b-1}\,\mathrm{d}x. \tag{53}$$

Equation (52) is equivalent to the corresponding expression obtained by Zigelman and Manor [26] [their equation (22)] in which, as previously mentioned, $J \equiv 1$. When $\text{Da} = 0$, there is no adsorption onto the substrate and so trivially $\phi_{\text{s}} \equiv 0$, while when $\text{Da} = 4/\pi$, ϕ_{s} is spatially uniform throughout the evaporation and is given by $\phi_{\text{s}} = (1-\theta)/4$. From (52), the final adsorbed deposit is given by

$$\phi_{\text{s, lifetime}} = \frac{\pi\,\text{Da}\left(1-r^2\right)^{-(1-\pi\,\text{Da}/4)}}{8r^{2(1+\pi\,\text{Da}/4)}} B_{r^2}\left(1+\frac{\pi\,\text{Da}}{4}, 2-\frac{\pi\,\text{Da}}{4}\right). \tag{54}$$

Figure 4 shows $\phi_{\text{s, lifetime}}$ given by (54) plotted as a function of r for various values of $\text{Da} > 0$. In particular, Fig. 4 shows that $\phi_{\text{s, lifetime}}$ has qualitatively the same spatial behaviour as that of ϕ shown in Figs. 2 and 3. Specifically, for $0 < \text{Da} < 4/\pi$, $\phi_{\text{s, lifetime}}$ is a monotonically increasing function of r that takes its minimum value at $r = 0$ and is singular at the contact line according to $\phi_{\text{s, lifetime}} = O\left((1-r)^{-(1-\pi\,\text{Da}/4)}\right) \to \infty$; for $\text{Da} = 4/\pi$, it is spatially uniform and is given by $\phi_{\text{s, lifetime}} \equiv 1/4$; and for $\text{Da} > 4/\pi$, it is a monotonically decreasing function of r that takes its maximum value at $r = 0$ and goes to zero at the contact line according to $\phi_{\text{s, lifetime}} = O\left((1-r)^{-(1-\pi\,\text{Da}/4)}\right) \to 0^+$. In other words, as Da increases a switch from a final adsorbed deposit that is more concentrated near to the contact line of the droplet to one that is more concentrated near to the centre of the droplet occurs at $\text{Da} = 4/\pi$, with $\phi_{\text{s, lifetime}} \to h(r, 0) = (1-r^2)/2$ as $\text{Da} \to \infty$.

Substituting the expressions for h and ϕ given by (13) and (51), respectively, into (43) and evaluating the integral yields an explicit expression for the mass of particles in the bulk of the droplet, namely

$$M_{\text{drop}} = M_0 \frac{2\theta^{(1+\pi\,\text{Da}/4)/2}}{1+\pi\,\text{Da}/4}\,{}_2F_1\left(1, -1+\frac{\pi\,\text{Da}}{4}; 2+\frac{\pi\,\text{Da}}{4}; \theta^{1/2}\right), \tag{55}$$

where $M_0 = \pi/4$ and ${}_2F_1(a, b; c; z)$ denotes the Gaussian (i.e. the ordinary) hypergeometric function.

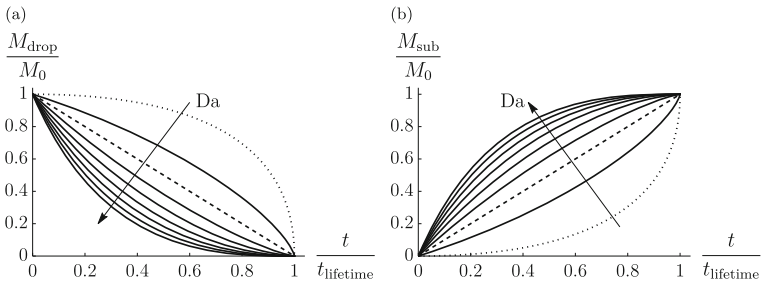

Fig. 5 The evolutions of **a** M_{drop}/M_0 given by (55) and **b** M_{sub}/M_0 given by (56) plotted as functions of t/t_{lifetime} for a droplet undergoing spatially uniform evaporation when $\text{Da} = (0, 1/2, \ldots, 4) \times 4/\pi$. The dotted and dashed lines correspond to $\text{Da} = 0$ and $\text{Da} = 4/\pi$, respectively. When $\text{Da} = 0$, $M_{\text{sub}} \equiv 0$, and so the dotted line in (**b**) shows M_{ring}/M_0 rather than M_{sub}/M_0. The arrows indicate the direction of increasing Da

Similarly, substituting the expression for ϕ_s given by (52) into (45) and evaluating the integral yields an explicit expression for the mass of particles adsorbed onto the substrate, namely

$$\begin{aligned} M_{\text{sub}} &= M_0 \left[1 - \frac{2\theta^{(1+\pi\text{Da}/4)/2}}{1+\pi\text{Da}/4} {}_2F_1\left(1, -1 + \frac{\pi\text{Da}}{4}; 2 + \frac{\pi\text{Da}}{4}; \theta^{1/2}\right) \right] \\ &= M_0 - M_{\text{drop}}. \end{aligned} \tag{56}$$

When $\text{Da} = 0$, $\phi_s \equiv 0$ and hence $M_{\text{sub}} \equiv 0$, and substituting the solution for ϕ given by (51) when $\text{Da} = 0$ into (43) and (46) and evaluating the integrals recovers the solutions for M_{drop} and M_{ring} in the absence of particle–substrate adsorption, namely

$$M_{\text{drop}} = M_0 \left[1 - \left(1 - \theta^{1/2}\right)^2 \right], \quad M_{\text{ring}} = M_0 \left(1 - \theta^{1/2}\right)^2 = M_0 - M_{\text{drop}} \tag{57}$$

(see, for example, D'Ambrosio et al. [22]), showing that in the absence of particle–substrate adsorption all of the particles initially in the bulk of the droplet are eventually advected to the contact line, where they form a final ring deposit of mass $M_{\text{ring}}(t_{\text{lifetime}}) = M_0$.

On the other hand, when $\text{Da} > 0$, equations (48) and (51) show that $\phi\, Q\, r \to 0^+$ as $r \to 1^-$ [see equation (A11) in Appendix A for the exact expression], and therefore (46) gives $M_{\text{ring}} \equiv 0$, showing that in the presence of particle–substrate adsorption, all of the particles initially in the bulk of the droplet are eventually adsorbed onto the substrate, where they form a (in general, spatially non-uniform) final adsorbed deposit of mass $M_{\text{sub}}(t_{\text{lifetime}}) = M_0$.

Figure 5 shows the evolutions of M_{drop}/M_0 given by (55) and M_{sub}/M_0 given by (56) plotted as functions of t/t_{lifetime} for various values of Da. In particular, Fig. 5a illustrates that for all values of $\text{Da} \geq 0$, M_{drop} decreases monotonically from M_0 at $t = 0$ to 0 at $t = t_{\text{lifetime}}$, and Fig. 5b illustrates that for $\text{Da} > 0$, M_{sub} increases monotonically from 0 at $t = 0$ to M_0 at $t = t_{\text{lifetime}}$, i.e. all of the particles initially in

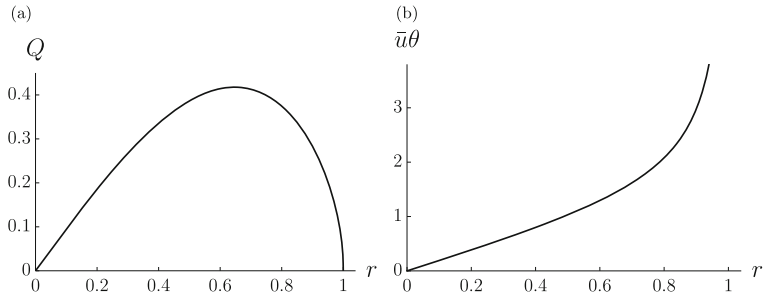

Fig. 6 **a** Q given by (58) and **b** $\bar{u}\theta$ given by (59) plotted as functions of r for a droplet undergoing diffusion-limited evaporation

the bulk of the droplet are eventually advected to the contact line when $\mathrm{Da} = 0$, but are eventually adsorbed onto the substrate when $\mathrm{Da} > 0$.

3.2 Diffusion-limited evaporation

Substituting the expressions for J and h given by (4) and (13), respectively, into (22) and evaluating the integral yields the familiar expressions for Q, and hence $\bar{u}$, for a thin droplet undergoing diffusion-limited evaporation,

$$Q = \frac{2}{\pi r}\left[(1-r^2)^{1/2} - (1-r^2)^2\right] \tag{58}$$

and

$$\bar{u} = \frac{4}{\pi r\theta}\left[(1-r^2)^{-1/2} - (1-r^2)\right] \tag{59}$$

(see, for example, Boulogne et al. [23], Gelderblom et al. [9], and D'Ambrosio et al. [22]). Figure 6 shows Q and $\bar{u}\theta$ (both of which are again independent of t) plotted as functions of r.

As in Sect. 3.1, substituting the expression for Q given by (58) into (42) and evaluating the integrals yields an implicit solution for ϕ (the details of which are omitted for brevity), and eliminating r_0 yields an explicit expression for the concentration of particles within a droplet undergoing diffusion-limited evaporation, namely

$$\begin{aligned}\phi = \frac{s}{\theta^{1/4}s_0}&\left[\frac{(1-s)^2(1+s_0+s_0^2)}{(1-s_0)^2(1+s+s^2)}\right]^{\pi\mathrm{Da}/12}\\ &\times\exp\left[\frac{\pi\mathrm{Da}}{2\sqrt{3}}\arctan\left(\frac{\sqrt{3}(s_0-s)}{2+s_0+s+2s_0s}\right)\right],\end{aligned} \tag{60}$$

where $s = s(r,t)$ is given by

$$s = \theta^{1/4}\left[\theta^{-3/4} - 1 + (1-r^2)^{3/2}\right]^{1/3}, \tag{61}$$

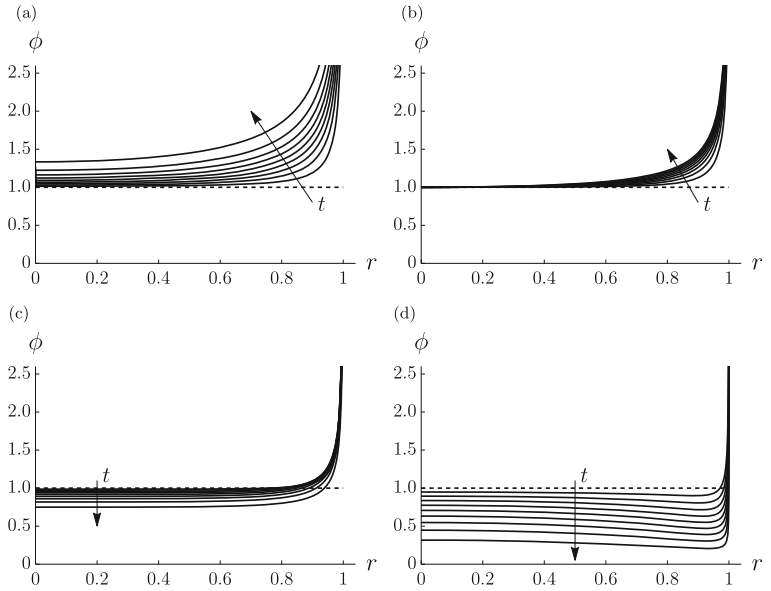

Fig. 7 The concentration of particles within the droplet ϕ given by (60) plotted as a function of r at times $t = (0, 1/10, \ldots, 9/10) \times t_{\text{lifetime}}$ for a droplet undergoing diffusion-limited evaporation when **a** $\text{Da} = 1/\pi$, **b** $\text{Da} = 2/\pi$, **c** $\text{Da} = 3/\pi$, and **d** $\text{Da} = 6/\pi$. The dashed lines correspond to the initial concentration $\phi \equiv 1$ at $t = 0$, and the arrows indicate the direction of increasing t

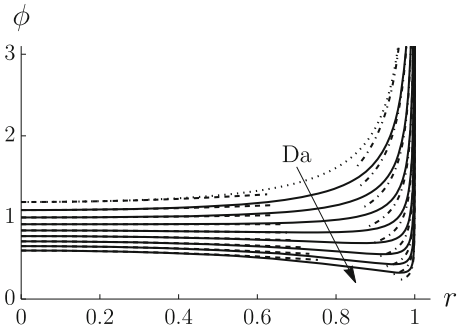

Fig. 8 The concentration of particles within the droplet ϕ given by (60) plotted as a function of r at $t = t_{\text{lifetime}}/2 = \pi/32$ for a droplet undergoing diffusion-limited evaporation when $\text{Da} = (0, 1/2, \ldots, 4) \times 2/\pi$. The dotted line corresponds to $\text{Da} = 0$, the dashed and dot-dashed lines correspond to the asymptotic expressions for ϕ near to the centre and near to the contact line of the droplet given by (64) and (65), respectively, and the arrow indicates the direction of increasing Da

and $s_0 = s(r, 0) = (1 - r^2)^{1/2}$. Setting $\text{Da} = 0$ in (60) again recovers the solution for ϕ in the absence of particle–substrate adsorption (see, for example, Zheng [19]).

Figures 7 and 8 show ϕ given by (60) plotted as a function of r at various times for (a) $\text{Da} = 1/\pi$ (typical of $0 \leq \text{Da} < 2/\pi$), (b) $\text{Da} = 2/\pi$, (c) $\text{Da} = 3/\pi$ (typical of $2/\pi < \text{Da} \leq 3/\pi$), and (d) $\text{Da} = 6/\pi$ (typical of $\text{Da} > 3/\pi$), and as a function of r at $t = t_{\text{lifetime}}/2 = \pi/32$ for various values of Da, respectively. In particular, Figs. 7

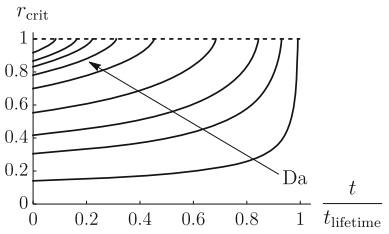

Fig. 9 Plot of r_{crit} given by (62) as a function of t/t_{lifetime} at $\text{Da} = (101/100, 21/20, 11/10, 6/5, 7/5, 8/5, 9/5, 2, 5/2) \times 2/\pi$. The dashed line corresponds to $r_{\text{crit}} = 1$ and the arrow indicates the direction of increasing Da

and 8 illustrate that, unlike for spatially uniform evaporation, ϕ is always singular at the contact line, and that the behaviour of ϕ is qualitatively different for $0 \leq \text{Da} < 2/\pi$, $\text{Da} = 2/\pi$, $2/\pi < \text{Da} \leq 3/\pi$, and $\text{Da} > 3/\pi$. Specifically, for $0 \leq \text{Da} \leq 3/\pi$, ϕ is a monotonically increasing function of r, but for $\text{Da} > 3/\pi$, ϕ first decreases to a minimum before increasing as a function of r. On the other hand, for $0 \leq \text{Da} \leq 2/\pi$, ϕ is an increasing function of t for all values of r (with $\phi(0, t) \equiv 1$ when $\text{Da} = 2/\pi$), but for $\text{Da} > 2/\pi$, ϕ is a decreasing function of t for $0 \leq r < r_{\text{crit}}$ and an increasing function of t for $r_{\text{crit}} < r \leq 1$, where $r_{\text{crit}} = r_{\text{crit}}(\text{Da}, t)$ is determined by solving the equation $\partial\phi/\partial t = 0$ for r to yield

$$r_{\text{crit}} = \sqrt{1 - \theta^{-1/2}\left[\theta^{3/4} - 1 + \left(\frac{2}{\pi\,\text{Da}}\right)^3\right]^{2/3}}. \tag{62}$$

Figure 9 shows r_{crit} given by (62) plotted as a function of t/t_{lifetime} for various values of $\text{Da} > 2/\pi$. In particular, Fig. 9 illustrates that r_{crit} is a monotonically increasing function of Da for $\text{Da} > 2/\pi$ that satisfies $r_{\text{crit}} \to 0^+$ as $\text{Da} \to (2/\pi)^+$ and $r_{\text{crit}} \to 1^-$ as $\text{Da} \to \infty$. Figure 9 also illustrates that r_{crit} is a monotonically increasing function of t for $0 \leq t \leq t_{\text{crit}}$ that satisfies $r_{\text{crit}} \to \sqrt{1 - (2/(\pi\,\text{Da}))^2}^+$ as $t \to 0^+$ and $r_{\text{crit}} \to 1^-$ as $t \to t_{\text{crit}}^-$, where $t_{\text{crit}} = t_{\text{crit}}(\text{Da})$ $(0 < t_{\text{crit}} < t_{\text{lifetime}})$ is given by

$$\frac{t_{\text{crit}}}{t_{\text{lifetime}}} = 1 - \left[1 - \left(\frac{2}{\pi\,\text{Da}}\right)^3\right]^{4/3}. \tag{63}$$

In particular, near to the centre of the droplet

$$\phi = \theta^{(-1+\pi\,\text{Da}/2)/4}\left[1 + \frac{r^2}{2}\left(1 - \frac{\pi\,\text{Da}}{3}\right)\left(1 - \theta^{3/4}\right)\right] + O\left(r^4\right) \tag{64}$$

as $r \to 0^+$, confirming the behaviour of ϕ near to the centre of the droplet described above. On the other hand, near to the contact line

$$\phi = \frac{s_1}{\theta^{1/4}}\left(\frac{(1 - s_1)^2}{1 + s_1 + s_1^2}\right)^{\pi\,\text{Da}/12} \exp\left[-\frac{\pi\,\text{Da}}{2\sqrt{3}}\arctan\left(\frac{\sqrt{3}s_1}{2 + s_1}\right)\right] \times \left(\frac{1}{\sqrt{2}\sqrt{1 - r}} + \frac{\pi\,\text{Da}}{2}\right) + O\left((1 - r)^{1/2}\right) \tag{65}$$

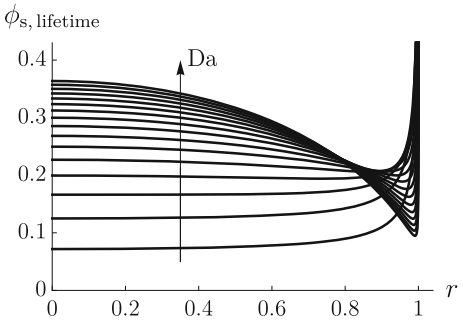

Fig. 10 The concentration of particles adsorbed onto the substrate at the end of the evaporation $\phi_{\text{s, lifetime}}$ given by (36) plotted as a function of r for a droplet undergoing diffusion-limited evaporation when $\text{Da} = (1/2, \ldots, 8) \times 2/\pi$. The arrow indicates the direction of increasing Da

as $r \to 1^-$, where $s_1 = s(1, t) = (1 - \theta^{3/4})^{1/3}$, confirming that ϕ is always singular at the contact line. Figure 8 includes dashed and dot-dashed lines corresponding to the asymptotic expressions for ϕ near to the centre and near to the contact line of the droplet given by (64) and (65), respectively.

Unlike for spatially uniform evaporation, the temporal integral of ϕ given by (60) has no closed-form analytical expression, and so the concentration of particles adsorbed onto the substrate ϕ_{s} given by (36) must be calculated numerically.

Figure 10 shows $\phi_{\text{s, lifetime}}$ given by (36) plotted as a function of r for various values of $\text{Da} > 0$. In particular, Fig. 10 shows that $\phi_{\text{s, lifetime}}$ is always singular at the contact line, and for $0 \leq \text{Da} \leq 3/\pi$, it is a monotonically increasing function of r, but for $\text{Da} > 3/\pi$, it first decreases to a minimum before increasing as a function of r, i.e. while there is always an adsorbed deposit near to the contact line, as Da increases the adsorbed deposit becomes increasingly more concentrated near to the centre of the droplet, and a switch from a local minimum to a local maximum in the concentration at the centre of the droplet occurs at $\text{Da} = 3/\pi$, and, as for spatially uniform evaporation, $\phi_{\text{s, lifetime}} \to h(r, 0) = (1 - r^2)/2$ as $\text{Da} \to \infty$. Using (64), it is possible to obtain an expression for ϕ_{s} near to the centre of the droplet, namely

$$\begin{aligned}\phi_{\text{s}} = \frac{\pi \text{Da}}{12\,(1 + \pi \text{Da}/6)} \Bigg[& 1 - \theta^{3(1+\pi \text{Da}/6)/4} \\ & + r^2 \frac{1 - \pi \text{Da}/3}{1 + \pi \text{Da}/4} \left(1 - \theta^{3(1+\pi \text{Da}/6)/4} \left\{ 2 + \frac{\pi \text{Da}}{2} - \left(1 + \frac{\pi \text{Da}}{6} \right) \theta^{3/4} \right\} \right) \Bigg] \\ & + O\left(r^4\right)\end{aligned} \tag{66}$$

as $r \to 0^+$, and hence

$$\phi_{\text{s, lifetime}} = \frac{\pi \text{Da}}{12\,(1 + \pi \text{Da}/6)} \left(1 + r^2 \frac{1 - \pi \text{Da}/3}{1 + \pi \text{Da}/4} \right) + O\left(r^4\right) \tag{67}$$

as $r \to 0^+$, confirming the behaviour of $\phi_{\text{s, lifetime}}$ near to the centre of the droplet described above.

Like ϕ_{s}, M_{drop}, M_{sub}, and M_{ring} given by (43), (45), and (46), respectively, must, in general, all be calculated numerically.

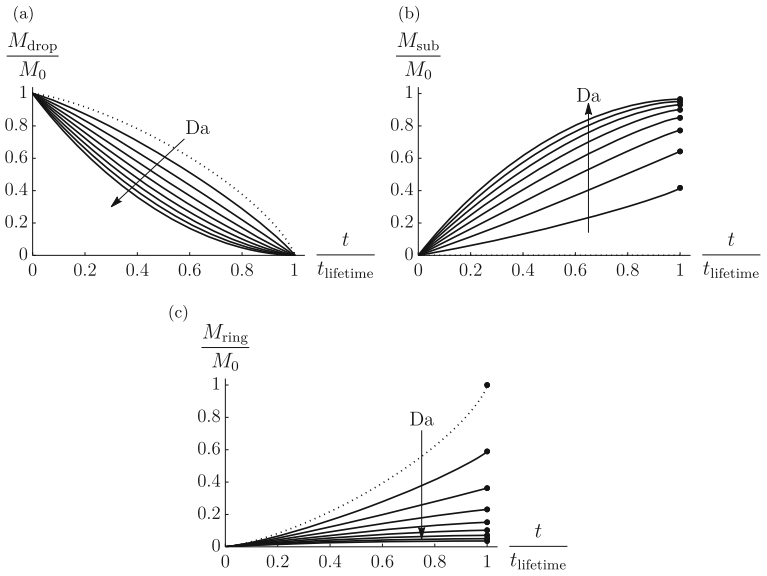

Fig. 11 The evolutions of **a** M_{drop}/M_0 given by (43), **b** M_{sub}/M_0 given by (45), and **c** M_{ring}/M_0 given by (46) plotted as functions of t/t_{lifetime} for a droplet undergoing diffusion-limited evaporation when $\text{Da} = (0, 1/2, \ldots, 4) \times 2/\pi$. The dotted lines correspond to $\text{Da} = 0$, the dots in (**b**) and (**c**) correspond to the values of $M_{\text{sub}}(t_{\text{lifetime}})/M_0$ and $M_{\text{ring}}(t_{\text{lifetime}})/M_0$, respectively, and the arrows indicate the direction of increasing Da

As for spatially uniform evaporation, when $\text{Da} = 0$, $\phi_s \equiv 0$ and hence $M_{\text{sub}} \equiv 0$, and substituting the solution for ϕ given by (60) when $\text{Da} = 0$ into (43) and (46) and evaluating the integrals recovers the solutions for M_{drop} and M_{ring} in the absence of particle–substrate adsorption, namely

$$M_{\text{drop}} = M_0\left[1 - \left(1 - \theta^{3/4}\right)^{4/3}\right], \quad M_{\text{ring}} = M_0\left(1 - \theta^{3/4}\right)^{4/3} = M_0 - M_{\text{drop}} \tag{68}$$

(see, for example, Deegan et al. [11] and D'Ambrosio et al. [22]), showing that in the absence of particle–substrate adsorption, all of the particles initially in the bulk of the droplet are eventually advected to the contact line, where they again form a final ring deposit of mass $M_{\text{ring}}(t_{\text{lifetime}}) = M_0$.

On the other hand, unlike for spatially uniform evaporation, when $\text{Da} > 0$, from equations (58) and (60) it may be shown that $\phi\, Q\, r = O(1)$ as $r \to 1^-$ [see equation (A12) in Appendix A for the exact expression], and therefore (46) gives $M_{\text{ring}} > 0$, showing that in the presence of particle–substrate adsorption not all of the particles initially in the bulk of the droplet are eventually adsorbed onto the substrate, and so the final deposit consists of a (in general, spatially non-uniform) final adsorbed deposit of mass $M_{\text{sub}}(t_{\text{lifetime}})$ and a final ring deposit of mass $M_{\text{ring}}(t_{\text{lifetime}}) = M_0 - M_{\text{sub}}(t_{\text{lifetime}})$.

Figure 11 shows the evolutions of M_{drop}/M_0 given by (43), M_{sub}/M_0 given by (45), and M_{ring}/M_0 given by (46) plotted as functions of t/t_{lifetime} for various val-

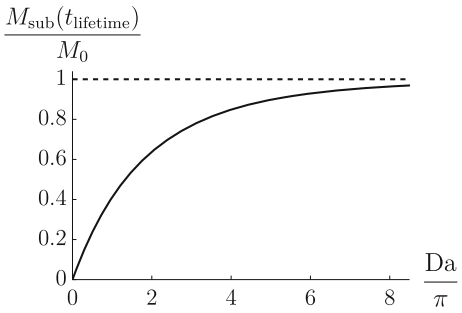

Fig. 12 $M_{\mathrm{sub}}(t_{\mathrm{lifetime}})/M_0$ plotted as a function of Da/π for a droplet undergoing diffusion-limited evaporation

ues of Da. In particular, Fig. 11a shows that, like for spatially uniform evaporation, for all values of $\mathrm{Da} \geq 0$, M_{drop} decreases monotonically from M_0 at $t = 0$ to 0 at $t = t_{\mathrm{lifetime}}$, and Figs. 11b, c show that M_{sub} and M_{ring} increase monotonically from 0 at $t = 0$ to $M_{\mathrm{sub}}(t_{\mathrm{lifetime}})$ and $M_{\mathrm{ring}}(t_{\mathrm{lifetime}})$, respectively, at $t = t_{\mathrm{lifetime}}$, i.e. all of the particles initially in the bulk of the droplet are eventually advected to the contact line when $\mathrm{Da} = 0$, but, unlike for spatially uniform evaporation, they are eventually either advected to the contact line or adsorbed onto the substrate when $\mathrm{Da} > 0$. Figures 11b, c also show, as might have been anticipated, that as Da increases, an increasing proportion of the particles are adsorbed onto the substrate, with $M_{\mathrm{sub}}(t_{\mathrm{lifetime}}) \to M_0^-$ and $M_{\mathrm{ring}}(t_{\mathrm{lifetime}}) \to 0^+$ as $\mathrm{Da} \to \infty$. This behaviour is illustrated in Fig. 12, which shows $M_{\mathrm{sub}}(t_{\mathrm{lifetime}})/M_0$ plotted as a function of Da/π.

Note that the present theoretical prediction of a final deposit consisting of an adsorbed deposit within the footprint of the droplet and a ring deposit at the contact line is in qualitative agreement with the experimental results of Devineau et al. [30], Anyfantakis et al. [31], and Bhardwaj et al. [32]. In particular, Anyfantakis et al. [31] showed that when the particles and substrate are oppositely charged, electrostatic particle–substrate attraction forces lead to a large number of particles being adsorbed onto the substrate within the footprint of the droplet, but that a ring deposit still occurs at the contact line due to the radially outward flow. Similarly, Bhardwaj et al. [32] observed that when the pH value of the fluid is decreased, the Derjaguin–Landau–Verwey–Overbeek (DLVO) forces present due to electrostatic and van der Waals forces cause particle–substrate attraction. As a result, the particles initially close to the substrate are attracted to, and form a layer of deposit on, the substrate. However, the DLVO forces are not sufficiently strong to attract all of the particles, and some of them are transported to the contact line by the radially outward flow to form a ring deposit. In addition, both of these studies showed that a switch from particle–substrate attraction to repulsion can be achieved by, for example, the addition of oppositely charged surfactant at sufficiently high concentrations (Anyfantakis et al. [31]) or increasing the pH value of the fluid (Bhardwaj et al. [32]), resulting in particles being transported to the contact line by the radially outward flow to form only a ring deposit.

4 Conclusions

In the present work we formulated and analysed a mathematical model for the evaporation of, the flow within, and the deposition from, a thin, pinned sessile droplet undergoing either spatially uniform or diffusion-limited evaporation. Specifically, we obtained explicit expressions for the concentration of particles within the bulk of the droplet, and described the behaviour of the concentration of particles adsorbed onto the substrate as well as the evolution of the masses within the bulk of the droplet, adsorbed onto the substrate, and in the ring deposit that can form at the contact line. The nature of the final deposit depends on the relative strengths of the depth-averaged radial velocity driven by evaporation that advects particles towards the contact line of the droplet and particle–substrate adsorption that adsorbs particles onto the substrate. In particular, we showed that, whereas for spatially uniform evaporation the presence of particle–substrate adsorption suppresses the formation of a ring deposit at the contact line and the final deposit consists of a (in general, spatially non-uniform) final adsorbed deposit of mass M_0, for diffusion-limited evaporation the final deposit consists of a (in general, spatially non-uniform) final adsorbed deposit of mass $M_{\text{sub}}(t_{\text{lifetime}})$ and a final ring deposit of mass $M_{\text{ring}}(t_{\text{lifetime}}) = M_0 - M_{\text{sub}}(t_{\text{lifetime}})$. The theoretical prediction of a final deposit consisting of an adsorbed deposit within the footprint of the droplet and a ring deposit at the contact line is in qualitative agreement with the experimental results of Devineau et al. [30], Anyfantakis et al. [31], and Bhardwaj et al. [32]. For both spatially uniform and diffusion-limited evaporation, the theoretically predicted final adsorbed deposit is more concentrated near to the contact line of the droplet when radial advection due to evaporation dominates particle–substrate adsorption, but is more concentrated near to the centre of the droplet when particle–substrate adsorption dominates radial advection due to evaporation. For spatially uniform evaporation, as Da increases, a switch from a final adsorbed deposit that is more concentrated near to the contact line of the droplet to one that is more concentrated near to the centre of the droplet occurs at $\text{Da} = 4/\pi$. In the special case $\text{Da} = 4/\pi$, the effects of radial advection and adsorption exactly cancel each other out, and so the concentration of particles remains at its spatially uniform and constant initial value throughout the evaporation. On the other hand, for diffusion-limited evaporation, while there is always a final adsorbed deposit near to the contact line (at which $\phi_{\text{s, lifetime}}$ is singular), as Da increases the final adsorbed deposit becomes increasingly more concentrated near to the centre of the droplet, and a switch from a local minimum to a local maximum in the concentration at the centre of the droplet occurs at $\text{Da} = 3/\pi$. In both scenarios, the final adsorbed deposit approaches a paraboloidal shape in the limit of strong particle–substrate adsorption. In addition, in Appendix A, we investigated the formation of a ring deposit at the contact line for a rather general form of the local evaporative flux, and showed that the presence of particle–substrate adsorption suppresses the formation of the ring deposit that can otherwise occur when the local evaporative flux is non-singular at the contact line.

It should, of course, be emphasised that the mathematical model considered in the present work is based on various simplifying assumptions, and future work could focus on relaxing these assumptions. For example, the particle-transport model in Sect. 2.3 considers the regime in which the vertical diffusion of particles within the droplet is

fast relative to the rate of evaporation and particle–substrate adsorption, i.e. $\hat{\theta}_0^2 \ll \mathrm{Pe}^* \ll 1$; however, it would also be of interest to explore the effect of radial particle diffusion within the droplet (see, for example, Moore et al. [21]) and to investigate the competition between particle diffusion and particle–substrate adsorption on the deposition from an evaporating droplet. It would also be of interest to further investigate the effect of particle–substrate adsorption on the deposition from non-thin droplets (see, for example, Masoud and Felske [51, 52]) and droplets with moving contact lines (see, for example, Freed-Brown [53]), as well as from non-axisymmetric droplets (see, for example, Sáenz et al. [54] and Wray and Moore [55]) and multiple evaporating droplets (see, for example, Wray et al. [47, 56]).

Appendix A The mass flux of particles into the contact line

In this Appendix, we investigate the formation of a ring deposit at the contact line for a rather general form of the local evaporative flux J, and show that the presence of particle–substrate adsorption suppresses the formation of the ring deposit that can otherwise occur when J is non-singular at the contact line.

For a general local evaporative flux of the form $J = J(r)$, the general expression for the local radial volume flux Q given by (22) may be written as

$$Q = \frac{I(1)H(r) - H(1)I(r)}{rH(1)}, \tag{A1}$$

in which $H = H(r)$ and $I = I(r)$ defined by

$$H = \int_0^r \eta(\tilde{r})\,\tilde{r}\,\mathrm{d}\tilde{r}, \quad I = \int_0^r J(\tilde{r})\,\tilde{r}\,\mathrm{d}\tilde{r} \tag{A2}$$

are the incomplete radial integrals of ηr and $J r$, respectively, where $\eta = \eta(r) = h(r,t)/\theta(t) = (1-r^2)/2$ is the spatial component of the free-surface profile given by (13) (see, for example, D'Ambrosio et al. [22]).

We assume that J has the rather general local form

$$J \sim J_n(1-r)^n \tag{A3}$$

as $r \to 1^-$, where $J_n\,(>0)$ is a strictly positive constant and the exponent n must satisfy $n > -1$ in order for J to be integrable, but is otherwise arbitrary, and so J is singular, finite and non-zero, and zero at the contact line for $-1 < n < 0$, $n = 0$, and $n > 0$, respectively.

Using $F = 4$, (A1), (A3), $H(r) = (2-r^2)r^2/8$, and $I(1) = F/(2\pi) = 2/\pi$, the local behaviour of Q near the contact line is

$$Q \sim \begin{cases} \dfrac{J_n}{n+1}(1-r)^{n+1} & \text{for} \quad -1 < n < 1 \\ \left(\dfrac{J_1}{2} - \frac{8}{\pi}\right)(1-r)^2 & \text{for} \quad n = 1 \\ -\dfrac{8}{\pi}(1-r)^2 & \text{for} \quad n > 1 \end{cases} \tag{A4}$$

as $r \to 1^-$ for all $\mathrm{Da} \geq 0$, and hence for $n > 1$ and for $J_1 < 16/\pi$ when $n = 1$, the local radial volume flux $Q\,(< 0)$ is directed away from the contact line, and so a ring deposit cannot form there, i.e. $M_{\mathrm{ring}} \equiv 0$. However, for $-1 < n < 1$ and for $J_1 > 16/\pi$ when $n = 1$, the local radial volume flux $Q\,(> 0)$ is directed towards the contact line, and so in the absence of particle–substrate adsorption, a ring deposit can form there, even when J is finite and non-zero ($n = 0$) or zero ($0 < n \leq 1$) at the contact line (see, for example, D'Ambrosio et al. [22] and Wilson and D'Ambrosio [10]).

However, as we shall now show, the presence of particle–substrate adsorption suppresses the formation of the ring deposit when $0 \leq n \leq 1$.

Using (42) and (A3), the local behaviour of the concentration of particles within the bulk of the droplet ϕ near the contact line when $\mathrm{Da} > 0$ is

$$\phi = O\left((1-r)^{-(n+1)}\right) \to \infty \quad \text{for} \quad -1 < n < 0, \tag{A5}$$

$$\phi = O\left((1-r)^{(\mathrm{Da}-J_0)/J_0}\right) \to \begin{cases} \infty & \text{for} \quad \mathrm{Da} < J_0 \\ O(1) & \text{for} \quad \mathrm{Da} = J_0 \\ 0^+ & \text{for} \quad \mathrm{Da} > J_0 \end{cases} \quad \text{for} \quad n = 0, \tag{A6}$$

and

$$\phi = O\left((1-r)^{-(n+1)} \exp\left[-\frac{(n+1)\mathrm{Da}}{n J_n}(1-r)^{-n}\right]\right) \to 0^+ \quad \text{for} \quad 0 < n \leq 1 \tag{A7}$$

as $r \to 1^-$. The mass flux of particles from the bulk of the droplet into the contact line is $\lim_{r\to 1^-} 2\pi\,\phi\,Q\,r$, and so, using (A4)–(A7), is given by

$$\lim_{r\to 1^-} 2\pi\,\phi\,Q\,r = O(1) \quad \text{for} \quad -1 < n < 0, \tag{A8}$$

$$\lim_{r\to 1^-} 2\pi\,\phi\,Q\,r = O\left((1-r)^{\mathrm{Da}/J_0}\right) \to 0^+ \quad \text{for} \quad n = 0, \tag{A9}$$

and

$$\lim_{r\to 1^-} 2\pi\,\phi\,Q\,r = O\left(\exp\left[-\frac{(n+1)\mathrm{Da}}{n J_n}(1-r)^{-n}\right]\right) \to 0^+ \quad \text{for} \quad 0 < n \leq 1 \tag{A10}$$

as $r \to 1^-$, and hence, using (46), $M_{\mathrm{ring}} \equiv 0$ for $0 \leq n \leq 1$, i.e. the presence of particle–substrate adsorption suppresses the formation of the ring deposit at the contact line that can otherwise occur when J is non-singular at the contact line.

In the case of spatially uniform evaporation treated in Sect. 3.1, $J \equiv 4/\pi$ is finite and non-zero at the contact line (corresponding to $J_0 = 4/\pi$ and $n = 0$),

$$2\pi\,\phi\,Q\,r = O\left((1-r)^{\pi\,\mathrm{Da}/4}\right) \to 0^{+} \tag{A11}$$

as $r \to 1^{-}$ when $\mathrm{Da} > 0$, and so, as we have already seen, particle–substrate adsorption suppresses the ring deposit that occurs when $\mathrm{Da} = 0$.

On the other hand, in the case of diffusion-limited evaporation treated in Sect. 3.2, $J = 2/(\pi(1-r^2)^{1/2})$ is singular at the contact line according to $J = O((1-r)^{-1/2}) \to \infty$ as $r \to 1^{-}$ (corresponding to $J_{-1/2} = \sqrt{2}/\pi$ and $n = -1/2$),

$$2\pi\,\phi\,Q\,r \sim \frac{4s_1}{\theta^{1/4}}\left(\frac{(1-s_1)^2}{1+s_1+s_1^2}\right)^{\pi\,\mathrm{Da}/12} \exp\left[-\frac{\pi\,\mathrm{Da}}{2\sqrt{3}}\arctan\left(\frac{\sqrt{3}s_1}{2+s_1}\right)\right] = O(1), \tag{A12}$$

where again $s_1 = s(1,t) = (1-\theta^{3/4})^{1/3}$, as $r \to 1^{-}$ when $\mathrm{Da} > 0$, and so, as we have already seen, particle–substrate adsorption reduces the mass of, but does not entirely suppress, the ring deposit that occurs when $\mathrm{Da} = 0$.

Acknowledgements The authors wish to thank Dr Brian R. Duffy, David Craig, and Henry T. Sharp (all University of Strathclyde) for insightful discussions regarding this work.

Author contributions H.-M.D'A. performed the original calculations in close collaboration with S.K.W. and A.W.W. S.K.W. prepared the final version of manuscript based on an initial draft by H.-M.D'A. H.-M.D'A. created all of the figures. All three authors reviewed, checked, and approved the final version of the manuscript prior to submission.

Funding H.-M.D'A. gratefully acknowledges financial support from the United Kingdom Engineering and Physical Sciences Research Council (EPSRC) via EPSRC Additional Funding for Mathematical Sciences Grant EP/W522521/1 via the University of Strathclyde.

Data availability The present study is purely theoretical and does not involve the generation or analysis of experimental data. All of the results reported in the present work can be reproduced from the equations detailed within the manuscript.

Declarations

Conflict of interest The authors report no conflict of interest.

References

1. Layani M, Gruchko M, Milo O, Balberg I, Azulay D, Magdassi S (2009) Transparent conductive coatings by printing coffee ring arrays obtained at room temperature. ACS Nano 3(11):3537–3542
2. Garcia-Cordero JL, Fan ZH (2017) Sessile droplets for chemical and biological assays. Lab Chip 17(13):2150–2166
3. Halls J (2005) Ink-jet printing of PLED displays. Inf Disp 21(2):10–15
4. Cazabat A-M, Guéna G (2010) Evaporation of macroscopic sessile droplets. Soft Matter 6(12):2591–2612
5. Erbil HY (2012) Evaporation of pure liquid sessile and spherical suspended drops: A review. Adv Coll Interface Sci 170(1–2):67–86
6. Brutin D, Starov V (2018) Recent advances in droplet wetting and evaporation. Chem Soc Rev 47(2):558–585
7. Giorgiutti-Dauphiné F, Pauchard L (2018) Drying drops. Eur Phys J E 41(3):32
8. Brutin D, Sefiane K (2022) Drying of complex fluid drops: Fundamentals and applications. Soft Matter Series, vol 14. Royal Society of Chemistry, London
9. Gelderblom H, Diddens C, Marin A (2022) Evaporation-driven liquid flow in sessile droplets. Soft Matter 18(45):8535–8553
10. Wilson SK, D'Ambrosio H-M (2023) Evaporation of sessile droplets. Annu Rev Fluid Mech 55:481–509
11. Deegan RD, Bakajin O, Dupont TF, Huber G, Nagel SR, Witten TA (2000) Contact line deposits in an evaporating drop. Phys Rev E 62(1):756–765
12. Larson RG (2014) Transport and deposition patterns in drying sessile droplets. AIChE J 60(5):1538–1571
13. Mampallil D, Eral HB (2018) A review on suppression and utilization of the coffee-ring effect. Adv Coll Interface Sci 252:38–54
14. Parsa M, Harmand S, Sefiane K (2018) Mechanisms of pattern formation from dried sessile drops. Adv Coll Interface Sci 254:22–47
15. Zang D, Tarafdar S, Tarasevich YY, Choudhury MD, Dutta T (2019) Evaporation of a droplet: From physics to applications. Phys Rep 804:1–56
16. Kolegov KS, Barash LYu (2020) Applying droplets and films in evaporative lithography. Adv Coll Interface Sci 285:102271
17. Shao X, Duan F, Hou Y, Zhong X (2020) Role of surfactant in controlling the deposition pattern of a particle-laden droplet: fundamentals and strategies. Adv Coll Interface Sci 275:102049
18. Popov YO (2005) Evaporative deposition patterns: Spatial dimensions of the deposit. Phys Rev E 71(3):036313
19. Zheng R (2009) A study of the evaporative deposition process: Pipes and truncated transport dynamics. Eur Phys J E 29(2):205–218
20. Kaplan CN, Mahadevan L (2015) Evaporation-driven ring and film deposition from colloidal droplets. J Fluid Mech 781:R2
21. Moore MR, Vella D, Oliver JM (2021) The nascent coffee ring: How solute diffusion counters advection. J Fluid Mech 920:A54
22. D'Ambrosio H-M, Wilson SK, Wray AW, Duffy BR (2023) The effect of the spatial variation of the evaporative flux on the deposition from a thin sessile droplet. J Fluid Mech 970:A1
23. Boulogne F, Ingremeau F, Stone HA (2017) Coffee-stain growth dynamics on dry and wet surfaces. J Phys Condens Matter 29(7):074001
24. Ozawa K, Nishitani E, Doi M (2005) Modeling of the drying process of liquid droplet to form thin film. Jpn J Appl Phys 44(6R):4229
25. Man X, Doi M (2016) Ring to mountain transition in deposition pattern of drying droplets. Phys Rev Lett 116(6):066101
26. Zigelman A, Manor O (2018) The deposition of colloidal particles from a sessile drop of a volatile suspension subject to particle adsorption and coagulation. J Colloid Interface Sci 509:195–208
27. Zigelman A, Manor O (2018) Simulations of the dynamic deposition of colloidal particles from a volatile sessile drop. J Colloid Interface Sci 525:282–290
28. Mills LM (2022) On the evolution of and the deposition from a thin annular droplet. MPhil Thesis, University of Strathclyde

29. Kim H, Boulogne F, Um E, Jacobi I, Button E, Stone HA (2016) Controlled uniform coating from the interplay of Marangoni flows and surface-adsorbed macromolecules. Phys Rev Lett 116(12):124501
30. Devineau S, Anyfantakis M, Marichal L, Kiger L, Morel M, Rudiuk S, Baigl D (2016) Protein adsorption and reorganization on nanoparticles probed by the coffee-ring effect: Application to single point mutation detection. J Am Chem Soc 138(36):11623–11632
31. Anyfantakis M, Geng Z, Morel M, Rudiuk S, Baigl D (2015) Modulation of the coffee-ring effect in particle/surfactant mixtures: The importance of particle-interface interactions. Langmuir 31(14):4113–4120
32. Bhardwaj R, Fang X, Somasundaran P, Attinger D (2010) Self-assembly of colloidal particles from evaporating droplets: Role of DLVO interactions and proposition of a phase diagram. Langmuir 26(11):7833–7842
33. Lee HH, Fu SC, Tso CY, Chao CYH (2017) Study of residue patterns of aqueous nanofluid droplets with different particle sizes and concentrations on different substrates. Int J Heat Mass Transf 105:230–236
34. Anyfantakis M, Baigl D, Binks BP (2017) Evaporation of drops containing silica nanoparticles of varying hydrophobicities: Exploiting particle-particle interactions for additive-free tunable deposit morphology. Langmuir 33(20):5025–5036
35. Yunker PJ, Still T, Lohr MA, Yodh AG (2011) Suppression of the coffee-ring effect by shape-dependent capillary interactions. Nature 476(7360):308–311
36. Yunker PJ, Lohr MA, Still T, Borodin A, Durian DJ, Yodh AG (2013) Effects of particle shape on growth dynamics at edges of evaporating drops of colloidal suspensions. Phys Rev Lett 110(3):035501
37. Ryu S-A, Kim JY, Kim SY, Weon BM (2017) Drying-mediated patterns in colloid-polymer suspensions. Sci Rep 7:1079
38. Widjaja E, Harris MT (2008) Particle deposition study during sessile drop evaporation. AIChE J 54(9):2250–2260
39. Siregar DP, Kuerten JGM, van der Geld CWM (2013) Numerical simulation of the drying of inkjet-printed droplets. J Colloid Interface Sci 392:388–395
40. Crivoi A, Duan F (2013) Elimination of the coffee-ring effect by promoting particle adsorption and long-range interaction. Langmuir 29(39):12067–12074
41. Crivoi A, Zhong X, Duan F (2015) Crossover from the coffee-ring effect to the uniform deposit caused by irreversible cluster-cluster aggregation. Phys Rev E 92(3):032302
42. Sung P-F, Wang L, Harris MT (2019) Deposition of colloidal particles during the evaporation of sessile drops: Dilute colloidal dispersions. Int J Chem Eng 2019:7954965
43. Ren J, Crivoi A, Duan F (2020) Disk-ring deposition in drying a sessile nanofluid droplet with enhanced Marangoni effect and particle surface adsorption. Langmuir 36(49):15064–15074
44. Erdem AK, Denner F, Biancofiore L (2024) Numerical analysis of the dispersion and deposition of particles in evaporating sessile droplets. Langmuir 40(26):13428–13445
45. Murisic N, Kondic L (2011) On evaporation of sessile drops with moving contact lines. J Fluid Mech 679:219–246
46. Wilson SK, Duffy BR (2022) Mathematical models for the evaporation of sessile droplets. In: Brutin D, Sefiane K (eds) Drying of complex fluid drops. Royal Society of Chemistry, London, Chap. 4, pp 47–67
47. Wray AW, Wray PS, Duffy BR, Wilson SK (2021) Contact-line deposits from multiple evaporating droplets. Phys Rev Fluids 6(7):073604
48. Elimelech M, Gregory J, Jia X, Williams RA (1995) Particle deposition and aggregation. Colloid and Surface Engineering Series. Butterworth-Heinemann, Oxford
49. Adamczyk Z (2002) Irreversible adsorption of particles. In: Tóth J (ed) Adsorption: Theory, modeling and analysis. Marcel Dekker, New York, pp 251–374
50. Wray AW, Papageorgiou DT, Craster RV, Sefiane K, Matar OK (2014) Electrostatic suppression of the "coffee stain effect". Langmuir 30(20):5849–5858
51. Masoud H, Felske JD (2009) Analytical solution for inviscid flow inside an evaporating sessile drop. Phys Rev E 79(1):016301
52. Masoud H, Felske JD (2009) Analytical solution for Stokes flow inside an evaporating sessile drop: spherical and cylindrical cap shapes. Phys Fluids 21(4):042102
53. Freed-Brown J (2014) Evaporative deposition in receding drops. Soft Matter 10(47):9506–9510
54. Sáenz PJ, Wray AW, Che Z, Matar OK, Valluri P, Kim J, Sefiane K (2017) Dynamics and universal scaling law in geometrically-controlled sessile drop evaporation. Nat Commun 8:14783
55. Wray AW, Moore MR (2023) Evaporation of non-circular droplets. J Fluid Mech 961:A11
56. Wray AW, Duffy BR, Wilson SK (2020) Competitive evaporation of multiple sessile droplets. J Fluid Mech 884:A45